

Combined Natural Convection and Surface Radiation in a Cavity with Sinusoidal Waviness

Lahcen El Moutaouakil, Mohammed Boukendil, Aziz Idrissi Bougrine

Cadi Ayyad University, Faculty of Sciences Semlalia, B.P. 2390, Marrakesh, Morocco

Corresponding Author; Lahcen El Moutaouakil

Abstract : In this paper, the finite volume method is combined with the discrete ordinate method to study numerically the natural convection coupled to surface radiation in a differentially heated rectangular cavity with sinusoidal waviness located on the cold wall. The cavity is filled with air $Pr = 0.71$. The focus is on the effect of the emissivity $0 \leq \varepsilon \leq 1$, the waviness amplitude $0 \leq \alpha \leq 0.7$ and the cavity aspect ratio $1 \leq A \leq 4$ on the flow structure and heat transfer characteristics for different Rayleigh numbers $10^3 \leq Ra \leq 10^6$. In order to observe the influence of these pertinent dimensionless parameters, streamlines, isotherms, convective and radiative Nusselt numbers, velocity and temperature profiles are plotted for different combinations of aforementioned parameters. The numerical work is carried out using an in-house CFD code written in FORTRAN. The global Nusselt number is found to increase with the amplitude α and the cavity aspect ratio.

Keywords - Sinusoidal waviness, Natural convection, Surface radiation, Amplitude, Aspect ratio.

Date of Submission: 01-10-2019

Date of acceptance: 16-10-2019

I. INTRODUCTION

The growing interest of natural convection in cavities is dictated by the presence of such a phenomenon in many technological applications, such as the design of solar collectors and heat exchangers, building energy components, chemical processes, nuclear power and the cooling of electrical units. The number and diversity of studies has led to a large and specialized bibliography reporting a wide range of analytical, numerical and experimental results. In most published studies, the different shaped enclosures (rectangular (El Moutaouakil et al. [1]), triangular (Cui et al. [2], Das et al. [3]), and trapezoidal (Shi et al. [4], Iachachene et al. [5])) are limited by smooth and regular surfaces.

On the other hand, it should be mentioned that wavy geometries are used in many engineering systems as a means of enhancing the convective heat transfer such as in micro-electronic devices, solar collectors and in refrigerators, etc. This justifies the presence of works in the literature in which cavities having wavy wall(s) have been considered. Adjlout et al. [6] studied the influence of the hot wall undulations on heat transfer in inclined square cavity. They used a sinusoidal wall with one and three undulations. Their results indicate a decrease in convective heat transfer compared to the square cavity. They also showed that the evolution of the Nusselt number depends strongly on the number of undulations and their amplitude. Das and Shohel [7] numerically studied the natural flow of air and heat transfer in a differentially heated cavity with two corrugated horizontal walls and two straight vertical surfaces. They found that the wavelength-amplitude ratio affects the local heat transfer, the flow field as well as the thermal field. Sabeur et al. [8] numerically studied the effect of non-uniform thermal boundary conditions on natural convection and heat transfer in a differentially heated rectangular cavity with wavy sidewalls. The results indicate that the cavity with three undulations seems to reduce more the overall heat transfer than the cavity with one undulation. Slimani et al. [9] numerically studied laminar natural convection in a wavy cavity. The hot wavy bottom wall and the cold straight top wall are kept isothermal. They found that the flow and the heat transfer are strongly affected by the undulations amplitude. The turbulent natural convection of air flow in an inclined square cavity with a hot wavy wall is investigated numerically by Aounallah et al. [10]. This study reveals that, contrary to the flow at laminar regime, the presence of the wavy wall increases the local Nusselt number. The effects of volumetric heat sources on natural convection heat transfer and flow structures in a wavy-walled enclosure are studied numerically by Oztop et al. [11]. Hasan et al. [12] conducted a numerical study of the natural convection in a differentially heated square enclosure with wavy sidewalls. The results show that increasing the undulations amplitude and their number reduces the heat transfer rate within the cavity. Natural convection in a square cavity in the presence of sinusoidal roughness on vertical walls was studied numerically by Yousaf and Usman [13]. The obtained results showed that the sinusoidal roughness considerably affects the hydrodynamic and the thermal behavior of the fluid. An analysis of the natural convective flow and the heat transfer of a micropolar fluid in a wavy differentially heated cavity has been performed by Gibanov et al. [14]. It is observed that an increase in the

undulations number leads to a decrease in the heat transfer rate at the wavy wall. Hatami and Jing [15] have combined a numerical and statistical method to find the best wavy profile for the bottom plate of a nanofluid-based direct absorber solar collector. In order to obtain the best geometry of the wavy surface for maximizing of heat transfer, several works have been accomplished considering enclosed cavity filled with nanofluid [16]. It has been shown once again that the heat transfer performance depends on the particular values assigned to geometrical parameters of the wavy-surface. Other works dealing with pure natural flow and heat transfer in different thermal systems are available: open cavities subjected to a uniform magnetic field [17], lid driven cavity [18], tridimensional cavity [19], wavy channels [20] and plates [21].

To date, there are many studies involving natural convection and surface radiation in smooth cavities, and no work has been done (as much known to author) on wavy wall cavities. In addition, in normal operating situations, thermal radiation is strongly coupled with natural convection and could significantly affect the flow structure and the heat transfer within the cavity. Among the first studies dealing with the coupling between natural convection and thermal radiation in closed cavities, we can mention the work of Larson and Viskanta [22]. Their results show that radiation plays a more important role than natural convection. Colomer et al. [23] studied the problem of three-dimensional natural convection in a differentially heated cubic cavity filled with air with or without the contribution of surface radiation. The numerical results obtained for $10^3 \leq Ra \leq 10^6$ show a significant contribution of the radiation to the increase of the heat transfers in the case where the air is considered as a transparent medium. The interaction between natural convection and surface radiation has been studied numerically by Alvarado et al. [24] in an inclined cavity heated and cooled by two opposite walls and isolated by the remaining walls. The results of this steady-state study indicate that the surface radiation significantly modifies the flow structure and the average heat transfer in the cavity. The interaction of surface radiation with laminar and turbulent natural convection in cavities of large aspect ratio (greater than 10) and different boundary conditions is analyzed by El Moutaouakil et al. [25]. For design purposes, the authors developed accurate correlations for average convective and radiative Nusselt numbers.

From the above literature survey, it can be concluded that the heat transfer performance and flow properties within wavy-walled enclosures depends significantly on the geometry parameters of the wavy surface (e.g., the undulations amplitude and their number). The main aim of this work is to supplement this existing work by analyzing the effect of another important parameter (e.g., surface radiation) on natural convection heat transfer inside a wavy enclosure.

II. STUDIED CONFIGURATION

The schematic diagram of the studied configuration is shown in figure 1. It consists of a differentially heated rectangular cavity with equidistantly sinusoidal roughness elements located on the cold wall. These elements and the cold wall are maintained at a cold temperature $T_c = 293K$. The dimensionless amplitude $\alpha = h/L$ (see figure 1) of the sinusoidal elements was varied from 0 (smooth cavity) to 0.8, and their number is fixed at $N = 6$. The opposite wall is hot with a temperature $T_H = T_c + \Delta T$ while the horizontal walls are insulated. The sinusoidal undulations were generated by using following mathematical relationships for the right wall : $X = 1 - \alpha|\sin(2\pi NY)|$.

The cavity is filled with air ($Pr = 0.71$) and the Rayleigh number is varied from 10^3 to 10^6 (laminar regime). The temperature T_H varies from 297K to 357K according to the value of the Rayleigh number. Well known, Boussinesq approximation, which is commonly used to express the dependence of density with temperature, is adopted. For radiative exchanges, the surfaces are considered gray-diffuse with the same emissivity ϵ . The air is assumed to be perfectly transparent. The dimensionless governing equations for conservation of mass, momentum, and energy are given by:

$$\frac{\partial U_i}{\partial X_i} = 0 \tag{1}$$

$$\frac{\partial U_i}{\partial \tau} + U_j \frac{\partial U_i}{\partial X_j} = -\frac{\partial P}{\partial X_i} + Pr(\Delta U_i + \delta_{i2} Ra\theta) \tag{2}$$

$$\frac{\partial \theta}{\partial \tau} + U_i \frac{\partial \theta}{\partial X_i} = \Delta \theta - \frac{\tau}{Pl} \left[4 \left(\frac{\theta}{T_R} + 1 \right)^4 - \int_0^{4\pi} I_R d\Omega \right] \tag{3}$$

Dimensionless quantities (solutions of equations 1-3) are related to dimension ones by :

$$X_i = \frac{x_i}{L}, U_i = \frac{u_i L}{\alpha}, \theta = \frac{T - T_c}{\Delta T}, I_R = \frac{i_R}{\sigma T_c^4} \tag{4}$$

The dimensionless parameters involved in these equations are given by:

$$Pr = \frac{\nu}{\alpha}, Ra = \frac{g\beta\Delta T}{\nu\alpha} L^3, Pl = \frac{k\Delta T}{\sigma T_C^4 L}, T_R = \frac{T_C}{\Delta T} \quad (5)$$

The dimensionless radiative intensity I_R is determined by solving the following Radiative Transfer Equation (RTE):

$$\xi_i \frac{\partial I_R}{\partial X_i} + \tau I_R = \frac{\tau}{4\pi} \left[(1 - \omega) I_{Rb} + \omega \int_0^{4\pi} I_R \cdot \Phi \cdot d\Omega' \right] \quad (6)$$

ξ_i ($i = 1, 2$ and 3) are the direction cosines. The scattering albedo ω and the optical thickness are set to be zero in this study (surface radiation). Φ and $I_{Rb} = 4 \left(\frac{\theta}{T_R} + 1 \right)^4$ are the scattering phase function and the dimensionless blackbody emission, respectively.

The thermal boundary conditions are:

$\theta = 0$ for the wavy cold walls, $\theta = 1$ on the right vertical wall and $\frac{\partial \theta}{\partial Y} = \epsilon \left[-\frac{Q_{Rinc}}{Pl} + \left(\frac{\theta}{T_R} + 1 \right)^4 \right]$ on the horizontal walls. Q_{Rinc} is the adimensional radiative heat flux incident on the wall. It is calculated by using the expression:

$$Q_{Rinc} = \int_{\vec{n} \cdot \vec{s}' < 0} I_R \cdot |\vec{n} \cdot \vec{s}'| d\Omega \quad (7)$$

The local and average convective and radiative Nusselt numbers on the heated wall are:

$$\begin{aligned} Nu_{LC}(Y) &= \frac{\partial \theta(Y)}{\partial X}, Nu_{LR}(Y) = \frac{Q_R(Y)}{Pl} \text{ and } Nu_{C \text{ or } R} \\ &= \int_0^1 Nu_{LC \text{ or } LR}(Y) dY \end{aligned} \quad (8)$$

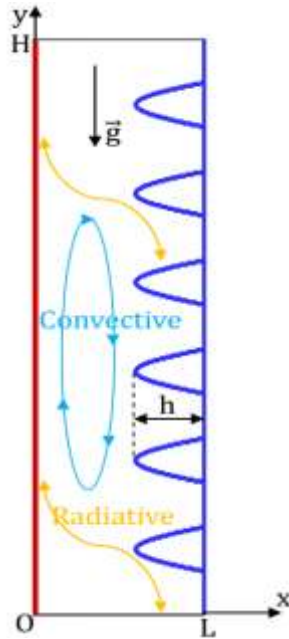


Figure 1. Studied configuration

III. NUMERICAL PROCEDURE AND VALIDATION

The governing equations of the studied problem are discretized by the finite volume method then solved by the SIMPLE algorithm. The equation (6) is integrated using the discrete ordinates method (DOM). A mesh testing procedure was conducted to guarantee the grid-independency of the present solution. As a result, it was found that a grid of 160×160 ensures a grid-independent solution. The developed numerical code was first validated for the case of pure natural convection in a differentially heated square cavity with the presence of roughness on its hot wall [13]. Table 1 compares the average Nusselt number obtained in the present simulation with previous study of Yousaf and Usman [13] by varying the amplitude α of the roughness elements from 0.025 to 0.15, Ra number from 10^3 to 10^6 while keeping the number N of roughness equal to 6. The obtained deviations are less than 1.81%.

Table 1. Nu_C for $N=6$ and different combinations (Ra,A)

| | | Yousaf and Usman [13] | | Present work | |
|----|--------|-----------------------|------|--------------|------|
| A | | 0.025 | 0.15 | 0.025 | 0.15 |
| Ra | 10^3 | 1.11 | 0.98 | 1.13 | 0.98 |
| | 10^4 | 2.22 | 1.66 | 2.25 | 1.64 |
| | 10^5 | 4.51 | 3.15 | 4.55 | 3.17 |
| | 10^6 | 8.77 | 6.28 | 8.82 | 6.31 |

In order to validate the accuracy of the code in the presence of surface radiation, a comparison was accomplished in the case of smooth square cavity ($A = 1$ and $\alpha = 0$) with other reference (Wang et al. [26]). The results are illustrated in figures 2 in terms of radiative Nusselt number profiles on the horizontal walls and the temperature along the vertical centerline of the cavity for $Ra = 10^6$ and different values of the emissivity. As can be clearly observed, there is a good agreement between our simulated results and those of Wang et al. [26].

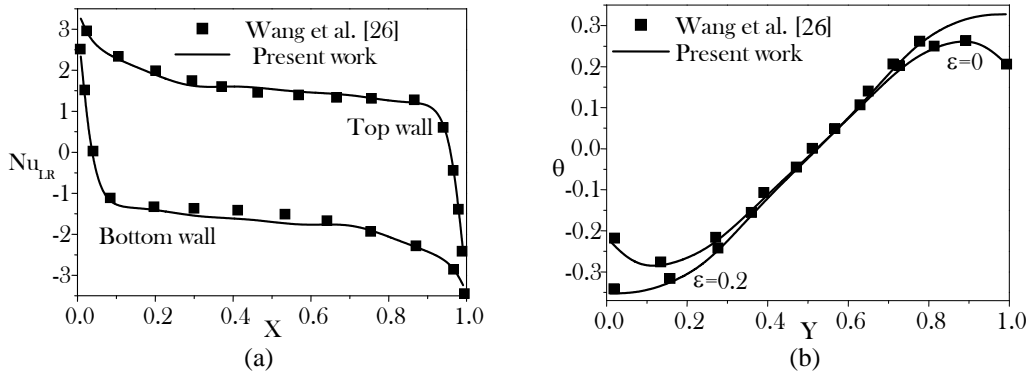


Figure 2. $Nu_{LR}(X)$ profiles on the horizontal walls for $\epsilon = 0.4$ and those of $\theta(Y)$ on the line $X = 0.5$ for different emissivities : $Ra = 10^6$

IV. RESULTS AND DISCUSSION

4.1 RAYLEIGH NUMBER AND EMISSIVITY EFFECTS

Figure 3 shows for $A = 1$, $\alpha = 0.4$ and different Ra numbers, the temperature of the horizontal passive walls $\theta(X)$ in the presence ($\epsilon = 1$) and in the absence ($\epsilon = 0$) of the surface radiation. From the figure, it can be seen that the temperature differences between the upper and the lower horizontal walls increase with the Ra number especially in the absence of surface radiation. For $Ra = 10^3$, the emissivity effect on $\theta(X)$ is limited and both horizontal walls have almost the same temperature. These temperatures decrease linearly for $X \leq 0.6$ indicating that the conduction is the dominant heat transfer mode in the cavity. The parts of the horizontal walls corresponding to $X \geq 0.6$ which are, therefore, of the same length as the sinusoidal elements are almost isothermal at $\theta = 0$. For $Ra = 10^6$, the surface radiation reduces significantly the difference between the passive wall temperatures by increasing the temperature of the lower surface and decreasing that of the upper wall. So, it can be concluded that the increase in emissivity leads to the reduction of the thermal stratification inside the cavity.

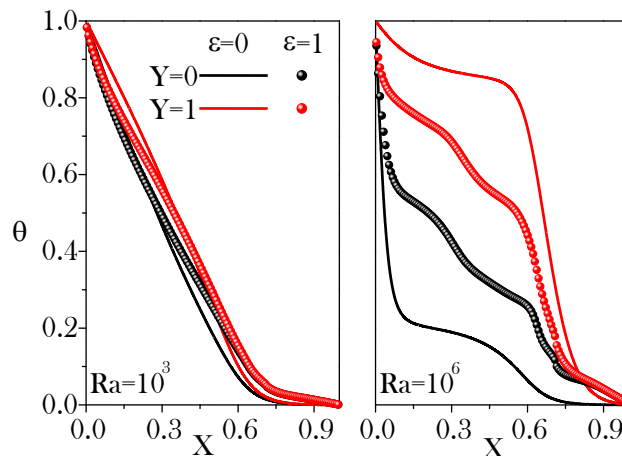


Figure 3. Passive wall temperatures for $A = 1$, $\alpha = 0.4$ and different combinations (ϵ, Ra)

Figure 4 shows under the same conditions as in figure 3, the horizontal velocity U and temperature variations along the vertical centerline of the cavity. For $Ra = 10^3$, the temperature profiles that are nearly vertical and the reduced U values show that the flow field is characterized by conduction dominant regime. The profiles corresponding to $\varepsilon = 0$ and $\varepsilon = 1$ are practically superimposed indicating that the emissivity has a limited effect for reduced Ra numbers. By switching to high Ra numbers, the radiation effect becomes more significant especially in the vicinity of the horizontal walls. By increasing the emissivity, temperature gradients in the vertical direction decrease, resulting in a less thermal stratification and velocity strengthening as it can be seen for $Ra = 10^6$. Note also that the velocity profiles have small amplitude undulations due to the presence of the sinusoidal waviness on the cold wall.

Variations in the local convective and radiative Nusselt numbers on the hot wall of the cavity are illustrated in the figure 5 for $A = 1$, $\alpha = 0.4$ and different combinations (Ra, ε). Depending on the considered Ra number, surface radiation can increase or reduce the local convective Nusselt number on the heated surface. For $Ra = 10^3$, the radiation considerably accentuates the convective exchanges at the hot wall ends, whereas for $Ra = 10^6$, a significant reduction of $Nu_{LC}(Y)$ is observed at the bottom of the hot wall. These changes at the hot wall ends are due to the passive walls whose temperatures are affected by the surface radiation (figure 5). Contrary to $Nu_{LC}(Y)$, the radiative profiles are practically symmetrical with respect to the center of the heated wall and do not change significantly with the Ra number. Note that the radiative contribution to the global heat transfer is seen to be more significant for the entire range of the Ra number.

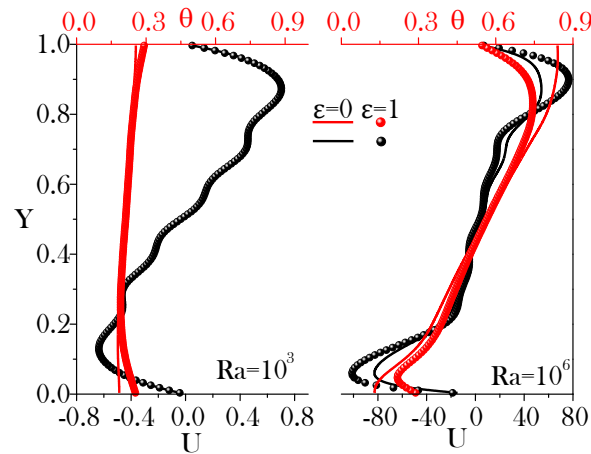


Figure 4. Profiles of $U(Y)$ and $\theta(Y)$ along the line $X=0.5$ for $A = 1$, $\alpha = 0.4$ and different combinations (Ra, ε)

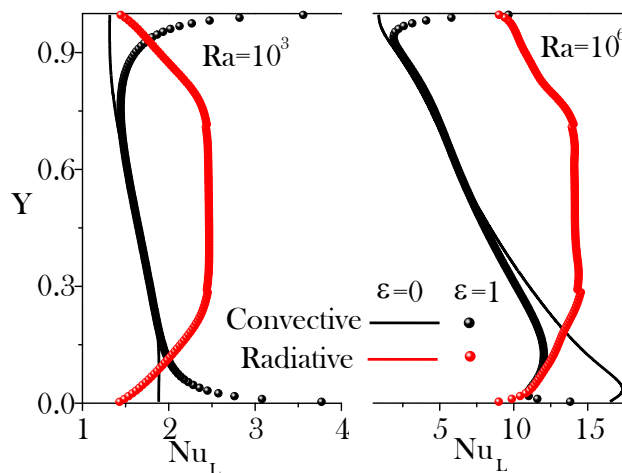


Figure 5. Profiles of $Nu_{LC}(Y)$ and $Nu_{LR}(Y)$ on the heated wall for different combinations (ε, Ra)

4.2 UNDULATION AMPLITUDE EFFECT

The undulations amplitude effect on the profiles of V (vertical velocity) and θ along the centerline $Y = 0.5$ is illustrated in figure 6 for $\varepsilon = 1$, $A = 1$, extreme Ra numbers and different amplitude α ranging from 0 (smooth cavity) to 0.8. This figure shows two distinct zones separated by the vertical line (L_v) passing through the ends of the sinusoidal elements. In the left part "zone1" of thickness α , the air is stagnant at a temperature $\theta \approx 0$. In the zone 2 (left of line L_v), the air rises along the hot wall ($V > 0$) and descends ($V < 0$) practically along

the line Lv. For $Ra = 10^3$, the velocity magnitude decreases considerably with α and the temperature decreases linearly from $X=0$ to $X=1-\alpha$ with a slope that increases with α . For $Ra = 10^6$, it can be seen that the extreme values of V are almost independent of the parameter α and that the temperature is almost uniform (equal to 0.5) in the central part of zone 2. This reflects the absence of interaction between ascending and descending thermal boundary layers formed along the isothermal walls.

The effect of the sinusoidal elements amplitude α on the local Nusselt number profiles along the heated wall is illustrated in figure 7 for $\epsilon = 1$, $A = 1$ and different Ra numbers. The local convective and radiative heat transfers increase with the amplitude α regardless of the Ra number value. This growth is clearly seen throughout the hot wall except for $Nu_{LC}(Y)$ leading for $Ra = 10^6$ to very close profiles on the upper half of the wall. Around the middle of the hot surface, the local radiative Nusselt number is almost uniform even in the presence of sinusoidal waviness on the cold one. Approaching the wall ends, $Nu_{LR}(Y)$ decreases to a minimum value that increases with α . Note also the amplitude α does not significantly alter the shape of the local convective and radiative Nusselt number profiles especially at low Ra numbers.

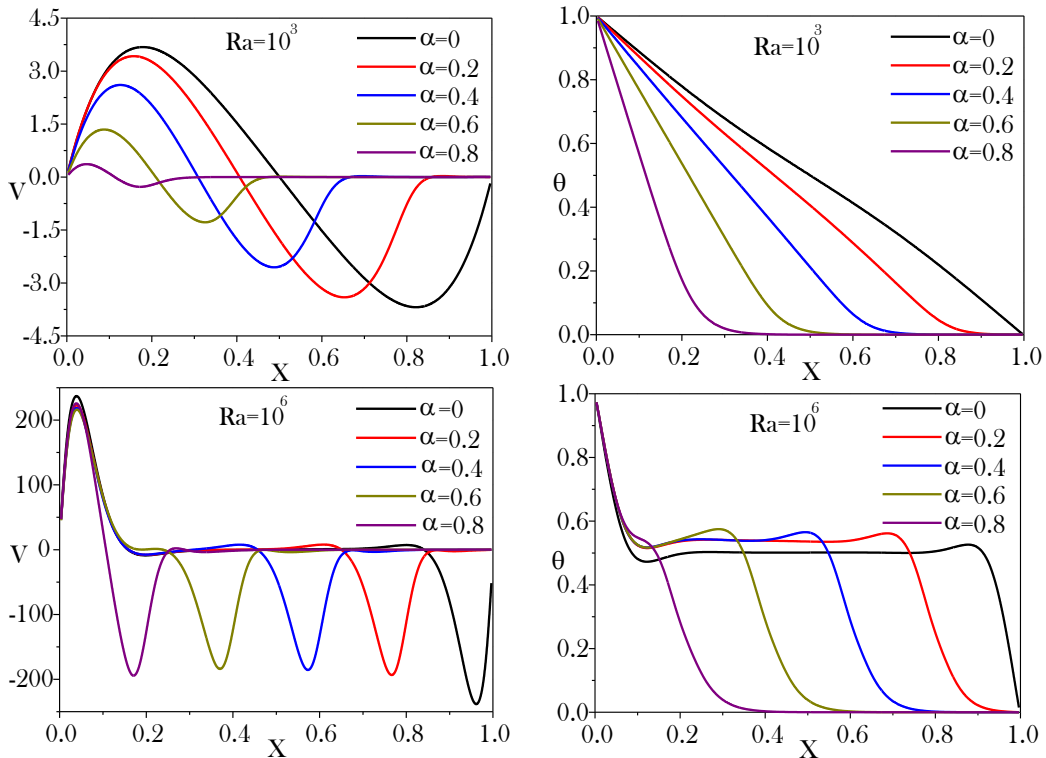
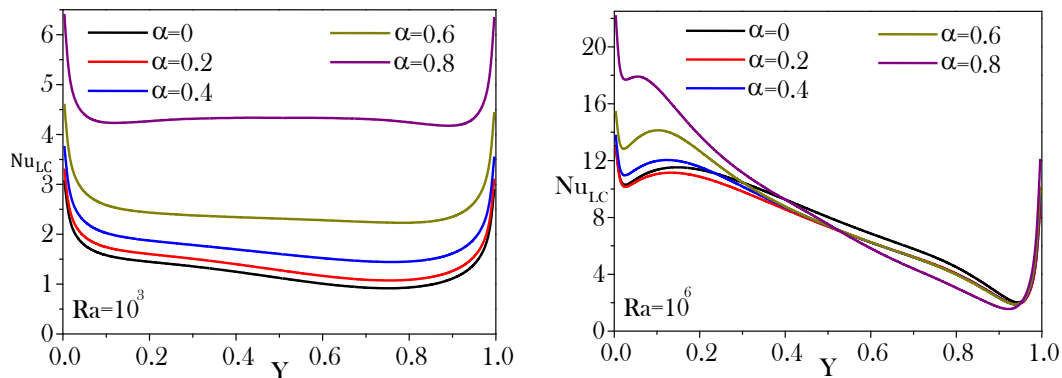


Figure 6. Profiles of $V(Y)$ and $\theta(Y)$ on the centerline $Y=0.5$ for $\epsilon = 1$, $A = 1$ and different combinations (α, Ra)



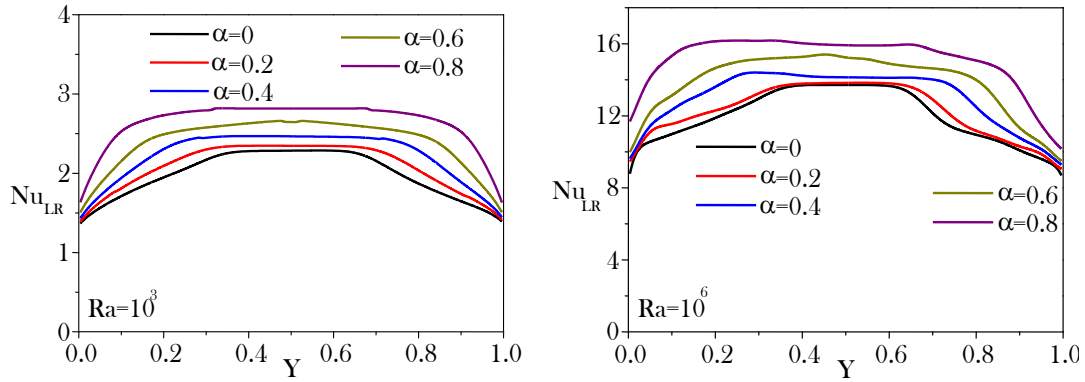


Figure 7. Profiles of $Nu_{LC}(Y)$ and $Nu_{LR}(Y)$ on the heated wall for $\varepsilon = 1$, $A = 1$ and different combinations (α, Ra)

4.3 ASPECT RATIO EFFECT

Figure 8 shows the streamlines and isotherms obtained for $Ra = 10^3$, $\varepsilon = 1$, $\alpha = 0.4$ and different aspect ratio A of the cavity. It can be shown that the flow and the thermal field are significantly affected due to the presence of sinusoidal waviness on the cold wall. The flow structure consists of a single clockwise cell occupying the entire cavity. The isothermal lines are nearly vertical showing that the conduction is the dominant mode of heat transfer in the cavity. For $A = 1$, the streamlines and isotherms touch only the undulations crest then move away from the cold wall trough indicating that the local Nusselt number distribution on the cold wall is higher near the crest and vanishes when approaching the wall trough. For $A = 4$, these lines penetrate a little more in the interstices of the sinusoidal elements and secondary disjoint cells (cat's eyes) appear in the central area of the cavity. This indicates that the waviness effect is more significant in tall cavities.

Figure 9 shows the streamlines and isotherms at $Ra = 10^6$, $\varepsilon = 1$, $\alpha = 0.4$ and different values of A . An increase in Ra leads to modification of both flow structure and position of isotherms inside the cavity. The isolines penetrate easily into the cold wall trough due to the flow strengthening especially for high values of A for which some interesting features of eddies or vortices formation between the sinusoidal elements were obtained. However, the heat transfer by conduction is still dominant in the stagnant central part of the cavity where the isotherms are nearly parallel to the horizontal walls for $A = 1$ and seen to have a negative slope for $A = 4$. Thus, the flow is less stable inside the tall cavities as it can be seen in figure 9. In the vicinity of the hot smooth wall, the thermal boundary layer thickness increases in the flow direction suggesting that the resulting local heat transfer will decrease along this wall.

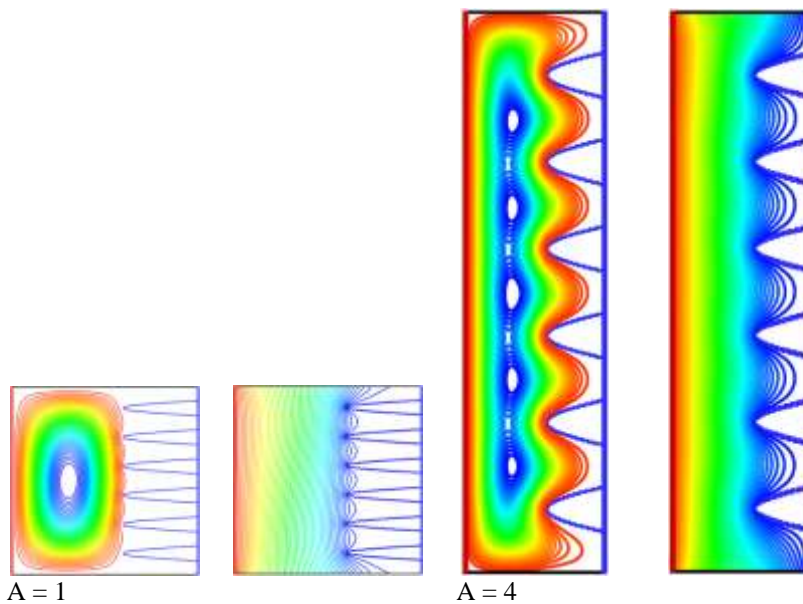


Figure 8. Streamlines and isotherms for $Ra = 10^3$, $\varepsilon = 1$, $\alpha = 0.4$ and different A

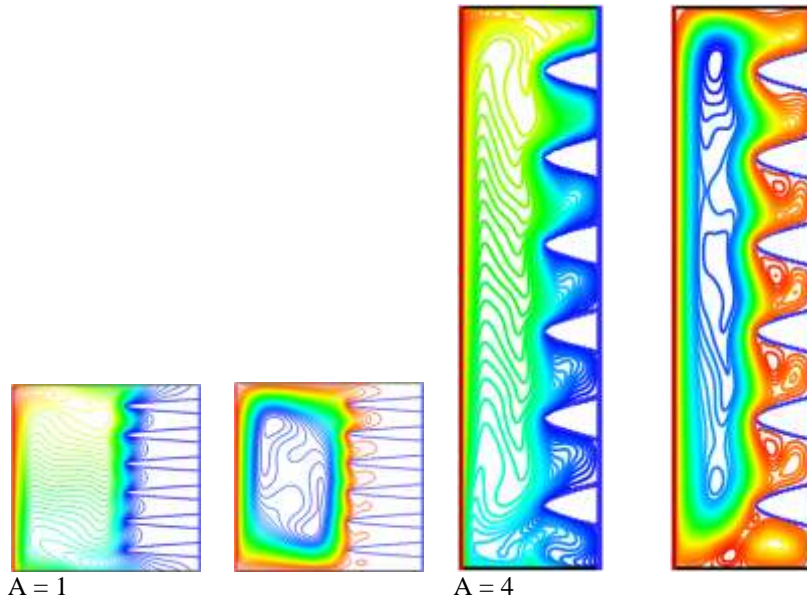


Figure 9. Streamlines and isotherms for $Ra = 10^6$, $\epsilon = 1$, $\alpha = 0.4$ and different A

Figure 10 represents the evolution of Nu_C and Nu_R as a function of α and Ra number for $\epsilon = 1$ and $A = 1$ (square cavity). The total Nu number can be easily calculated by: $Nu_T = Nu_C + Nu_R$. As expected, the convective and total Nusselt numbers increase rapidly with the Ra number especially beyond $Ra = 10^4$ (convective regime). It is interesting to note that both convective and radiative Nusselt numbers increase considerably with the undulations amplitude α especially at low Ra numbers for the convective Nusselt number and at high values of Rayleigh number for the radiative one. For $Ra = 10^6$, a slight decrease of Nu_C is observed between $\alpha = 0$ and $\alpha = 0.2$. A flow blocking effect is a possible explanation of the observed reduction. The proximity effect, which is better manifested in the conduction regime, explains the rapid growth of Nu_C for $Ra \leq 10^4$ and $\alpha \geq 0.6$.

Figure 11 represents the evolution of the convective and the radiative average Nusselt numbers (Nu_C, Nu_R) as a function of A and Ra number for $\epsilon = 1$ and $\alpha = 0.4$. It can be seen that the convective Nusselt number decrease linearly with α and conversely for the average radiative Nusselt number. The decline of Nu_C can be attributed to the thermal saturation of the air on the isothermal tall walls while the growth of Nu_R can be explained by the reduced passive walls contribution at high A values. It should be mentioned that, for $Ra = 10^6$, the radiation contributes more than 63% and 70% for $A = 1$ and $A = 4$, respectively. As a result, the overall heat transfer increases with the aspect ratio of the cavity over the entire range of the Rayleigh number.

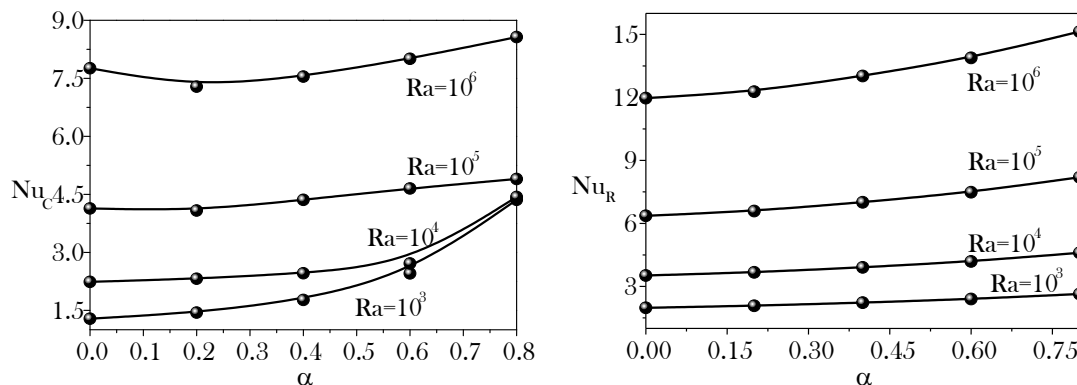


Figure 10. Profiles of Nu_C and Nu_R versus α for $A = 1$, $\epsilon = 1$ and different Ra numbers

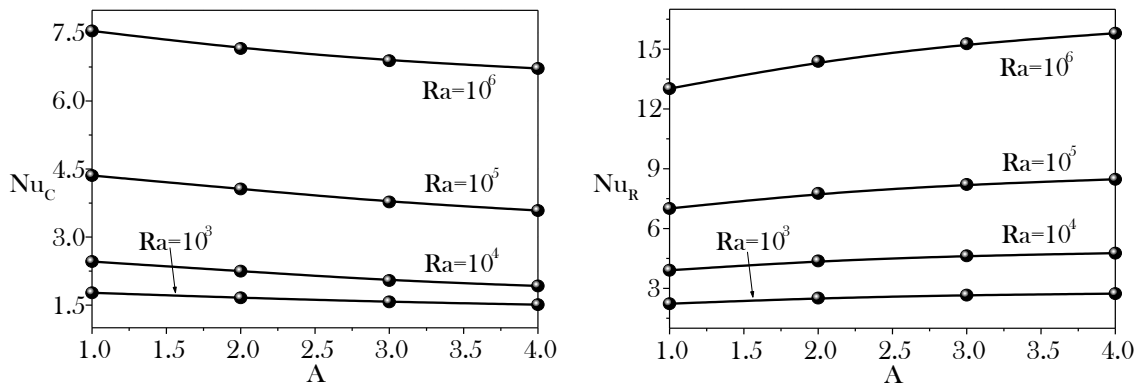


Figure 11. Profiles of Nu_C and Nu_R versus A for $\alpha = 0.4$, $\varepsilon = 1$ and different Ra numbers

V. CONCLUSION

A two-dimensional numerical analysis is carried out to explore the coupling between natural convection and surface radiation in a differentially heated cavity with sinusoidal waviness on its cold wall. Effects of dimensionless groups representing the sinusoidal elements amplitude, Rayleigh number, the aspect ratio of the cavity and the emissivity were highlighted to study their impacts on the flow structure and the heat transfer characteristics. The obtained results indicate that the increase of the emissivity reduces the thermal stratification and accentuates the flow intensity within the cavity. Moreover, results of this investigation have illustrated that both convective and radiative heat transfers increase with the amplitude of the sinusoidal elements. Thus, it can be concluded that non-smooth active walls are useful in promoting the heat transfer mechanisms in thermal systems. The results have also demonstrated that the streamlines and isotherms penetrate easily into the wall trough when the aspect ratio of the cavity is sufficiently large. In addition, obtained results indicate that convective Nusselt number decreases with aspect ratio of the cavity and conversely for the radiative Nusselt number.

REFERENCES

- [1]. L. El Moutaouakil, Z. Zrikem and A. Abdelbaki, Analytical and numerical study of natural convection induced by a volumetric heat generation in inclined cavities, *Applied Mathematical Modelling*, 40(40), 2016, 2913-2928.
- [2]. H. Cui, F. Xu and S.C. Saha, A three-dimensional simulation of transient natural convection in a triangular cavity, *International Journal of Heat and Mass Transfer*, 85, 2012, 1012-1022.
- [3]. D. Das, L. Lukose and T. Basak, Role of multiple solar heaters along the walls for the thermal management during natural convection in square and triangular cavities, *Renewable Energy*, 121, 2018, 205-229.
- [4]. D. Shi, G. Liu, H. Zhang, W. Ren and Q. Wang, A three-dimensional modeling method for the trapezoidal cavity and multi-coupled cavity with various impedance boundary conditions, *Applied Acoustics*, 154, 2019, 213-225.
- [5]. F.Z. Iachachene, H.F. Oztop and E. Abu-Nada, Melting of phase change materials in a trapezoidal cavity: Orientation and nanoparticles effects, *Journal of Molecular Liquids*, 292, 2019, 110592.
- [6]. L. Adjlout, O. Imine, A. Aziz and M. Belkadi, Laminar natural convection in an inclined cavity with a wavy wall, *International Journal of Heat and Mass Transfer*, 45(10), 2002, 2141-2152.
- [7]. P.K. Das and M. Shohel, Numerical investigation of natural convection inside a wavy enclosure, *International Journal of Thermal Sciences*, 42(4), 2003, 397-406.
- [8]. B.A. Sabeur, L. Adjlout and O. Imine, Effect of sinusoidal distribution of the temperature on laminar natural convection in wavy rectangular enclosures, *Journal of Applied Sciences*, 6(3), 2006, 710-715.
- [9]. A. Slimani, M. Rebhi, A. Belkacem and K. Bouhadeh, Natural convection in a horizontal wavy enclosure, *Journal of Applied Sciences*, 7(3), 2007, 334-341.
- [10]. M. Aounallah, Y. Addad, S. Benhamadouch, O. Imine, L. Adjlout and D. Laurence, Numerical investigation of turbulent natural convection in an inclined square cavity with a hot wavy wall, *International Journal of Heat and Mass Transfer*, 50(9-10), 2007, 1683-1693.
- [11]. H.F. Oztop, E. Abu-Nada, Y. Varol and A. Chamkha, Natural convection in wavy enclosures with volumetric heat sources, *International Journal of Thermal Sciences*, 50(4), 2011, 502-514.
- [12]. M.N. Hasan, S.C. Saha and Y.T. Gu, Unsteady natural convection within a differentially heated enclosure of sinusoidal corrugated side walls, *International Journal of Heat and Mass Transfer*, 55(21-22), 2012, 5696-5708.
- [13]. M. Yousaf and S. Usman, Natural convection heat transfer in a square cavity with sinusoidal roughness elements, *International Journal of Heat and Mass Transfer*, 90, 2015, 180-190.
- [14]. N.S. Gibanov, M.A. Sheremet and I. Pop, Natural convection of micropolar fluid in a wavy differentially heated cavity, *Journal of Molecular Liquids*, 221, 2016, 518-525.
- [15]. M. Hatami and D. Jing, Optimization of Wavy Direct Absorber Solar Collector (WDASC) using Al_2O_3 -water Nanofluid and RSM analysis, *Applied Thermal Engineering*, 121, 2017, 1040-1050.
- [16]. A.I. Alsabery, R. Mohebbi, A.J. Chamkha and I. Hashim, Effect of local thermal nonequilibrium model on natural convection in a nanofluid-filled wavy-walled porous cavity containing inner solid cylinder, *Chemical Engineering Science*, 201, 2019, 247-263.
- [17]. H.R. Ashorynejad and A. Shahriari, MHD natural convection of hybrid nanofluid in an open wavy cavity, *Results in Physics*, 9, 2018, 440-455.
- [18]. C.C. Cho, Mixed convection heat transfer and entropy generation of Cu-water nanofluid in wavy-wall lid-driven cavity in presence of inclined magnetic field, *International Journal of Mechanical Sciences*, 151, 2019, 703-714.

- [19]. F. Zemani, B.A. Sabeur and M. Boussoufi, Numerical investigation of natural convection in air filled cubical enclosure with hot wavy surface and partial partitions, *Procedia Computer Science*, 32, 2014, 622-630.
- [20]. F.B. Abdul Hasis, P.M. Mithun Krishna, G.P. Aravind, M. Deepu and S.R. Shine, Thermo hydraulic performance analysis of twisted sinusoidal wavy microchannels, *International Journal of Thermal Sciences*, 128, 2018, 124-136.
- [21]. C.Y. Cheng, Natural convection heat transfer from an inclined wavy plate in a bidisperse porous medium, *International Communications in Heat and Mass Transfer*, 43, 2013, 69-74.
- [22]. D.W. Larson and R. Viskanta, Transient combined laminar free convection and radiation in a rectangular enclosure, *Journal of Fluid Mechanics*, 78(1), 1976, 65-85.
- [23]. G. Colomer, M. Costa, R. Consul and A. Oliva, Three-dimensional numerical simulation of convection and radiation in a differentially heated cavity using the discrete ordinates method, *International Journal of Heat and Mass Transfer*, 47(2), 2004, 257-269.
- [24]. R. Alvarado, J. Xaman, J. Hinojosa and G. Alvarez, Interaction between natural convection and surface thermal radiation in tilted slender cavities, *International Journal of Thermal Sciences*, 47(4), 2008, 355-368.
- [25]. L. El Moutaouakil, Z. Zrikem and A. Abdelbaki, Interaction of surface radiation with laminar and turbulent natural convection in tall vertical cavities : analysis and heat transfer correlations, *Heat Transfer Engineering*, 36(17), 2015, 1472-1484.
- [26]. H. Wang, S. Xin and P. Le Quéré, Étude numérique du couplage de la convection naturelle avec le rayonnement de surfaces en cavité carrée remplie d'air, *Comptes Rendus Mécanique*, 334(1), (2006) 48-57.

Lahcen El Moutaouakil" Combined Natural Convection and Surface Radiation in a Cavity with Sinusoidal Waviness" *International Journal of Engineering Science Invention (IJESI)*, Vol. 08, No.10, 2019, PP 40-49